

List-driven source photometry in HIPE: feasibility study

Document number SPIRE-SUX-REP-003273

Anthony Smith (University of Sussex)

20th April 2012

1 Introduction

The purpose of this document is to explore the feasibility and cost of producing a HIPE implementation of existing linear inversion methods for the simultaneous estimation of source flux densities in crowded fields.¹ The methods currently exist in languages other than Java.

2 The methods

2.1 HerMES (Roseboom)

A method for list-driven photometry has been implemented by [Roseboom et al. \(2010\)](#) for the HerMES project. The basic approach is that the data (image), \mathbf{d} , is a combination of signal from sources and noise

$$\mathbf{d} = \mathbf{A}\mathbf{f} + \boldsymbol{\delta} \quad (1)$$

where \mathbf{A} is the pointing matrix, describing how the signal from point sources at known positions, each with a flux density of 1.0, is distributed on the image, \mathbf{f} is the vector of source flux densities, and $\boldsymbol{\delta}$ is the noise vector, giving the noise for each pixel. The pointing matrix is assumed to be known, and the noise is assumed to be Gaussian. Then the task is to find the maximum likelihood value for the flux densities, $\hat{\mathbf{f}}$. By representing the likelihood as a Gaussian, this is found to be

$$\hat{\mathbf{f}} = (\mathbf{A}^T \mathbf{N}_d^{-1} \mathbf{A})^{-1} \mathbf{A}^T \mathbf{N}_d^{-1} \mathbf{d} \quad (2)$$

where \mathbf{N}_d is the covariance matrix of the data (typically the noise in each pixel is assumed to be independent of the noise in the other pixels, so this is a simple diagonal matrix).

The method used for HerMES also imposes a constraint on the flux densities (that they must all be non-negative), making use of a bounded-variable least squares (BVLS) method. Additional features of the HerMES method involve filtering the list of “known” positions to remove sources that are not needed in order to give a good fit (using Bayesian model selection). However, having consulted with Isaac Roseboom, his recommendation for a generic task for inclusion in HIPE is to perform only the simple matrix inversion (e.g., using a conjugate gradient code), without the model selection or the positive prior on the flux density.

Challenges would be (1) developing a suitable method for dividing up the map into manageable segments, and (2) dealing with cases where sources are very close to each other (less than one pixel), and therefore would be highly correlated.

Note that background measurement (for each local segment) can easily be performed, simply by adding an extra “source”, which distributes its signal equally over all pixels in the map (or segment).

Uncertainties in the flux densities are given by the covariance matrix of flux densities, \mathbf{N}_f , which is estimated by $(\mathbf{A}^T \mathbf{N}_d^{-1} \mathbf{A})^{-1}$ ([Roseboom et al., 2010](#), equation 5). (Strictly, this is a lower limit to the covariance matrix, but it is computationally very challenging to improve on this estimate.) Since it is not safe to assume that correlations between source flux densities will be negligible, the implementation of the algorithm would need to take this into account, and provide the users with access to the information about the covariances in a suitable way.

¹<http://herschel.esac.esa.int/jira/browse/HCSS-14928>

2.2 PEP (Magnelli)

Berta et al. (2010) used simultaneous guided extraction for PACS photometry as part of the PEP project. The method used was that of Magnelli et al. (2009). Prior information is used, in the form of expected positions of the sources from mid-infrared data, and the method allows blending issues to be resolved to a large extent. Magnelli has confirmed by email that the core of his method is the same as that of Roseboom, with the same matrix inversion; the main differences are related to the optimisation of the catalogues of prior positions and the noise measurements.

2.3 BLAST (B  thermin)

B  thermin et al. (2010) used prior positions to derive flux densities on BLAST data using a PSF-fitting method. The method used is the same matrix inversion described above, using either the matrix inversion built into IDL, or a conjugate gradient method.²

2.4 SCUBA (Scott)

Scott et al. (2002, appendix A) used the same matrix inversion method on SCUBA data.

2.5 BLAST and LABOCA (Chapin)

Chapin et al. (2011) performed a joint analysis of BLAST and LABOCA data. As described in section 4.1, the used method was that described by Scott et al. (2002).

2.6 MADmap

MADmap uses a matrix inversion method identical to that of Equation (2).³ With MADmap already implemented in HIPE, one option would be to adapt MADmap to perform list-driven photometry, as described above.

However, there are some differences, which would make this both challenging and unnecessarily sophisticated. First, the assumptions about the noise are more sophisticated in MADmap, taking into account the Fourier transform of the noise properties of each detector. This is more than is needed for the (simpler) problem being considered. Moreover, the method proposed here takes the map as the data and solves to find the flux densities of the point sources, whereas MADmap takes the bolometer samples as the data and solves to find the map. Hence it is likely that significant alterations would be needed to adapt MADmap to this problem. (If the proposal was to use the bolometer samples to estimate the source flux densities, then there might be more sense in adapting the existing MADmap code, but that is not the current proposal.)

2.7 Summary of methods

The recommendation from this survey of possible methods is to implement the simpler version of the method used for HerMES, as described in Section 2.1. The following section is a demonstration of a prototype implementing this method.

3 HIPE Prototype

A prototype has been implemented as a Jython script in HIPE, to perform the simple matrix inversion, using built-in routines from the numerics package for matrix inversion and solution of matrix equations (which themselves use the JAMA package.⁴

An image with dimensions (50, 50) is created and Gaussian sources with a FWHM of 3.0 pixels are placed at random in this image, with their flux densities between 10.0 and 100.0 mJy, chosen at random from a uniform distribution in log-space. In the first test, the density is 0.1 sources per beam, and in the

²FASTPHOT on <http://www.ias.u-psud.fr/irgalaxies/downloads.php>

³<http://crd-legacy.lbl.gov/~cmc/MADmap/doc/introduction.html>

⁴<http://math.nist.gov/javanumerics/jama/>

second test, the density is 1.0 sources per beam. Source positions are random, and are not constrained to the centres of the pixels.

With the known source positions, the source fluxes are found first using the list-driven photometry method described above, and then using SUSSEXtractor.

This is performed both with and without noise added to the images. The images have units of mJy/beam, and the noise level is 5.0 mJy/beam, with Gaussian random noise per pixel.

Figure 1 shows the low-density images (0.1 sources per beam). 24 sources are in the images. Figure 2 shows the results for the low-density image without noise, while Figure 3 shows the results for the low-density image with noise.

Figure 4 shows the high-density images (1.0 sources per beam). 245 sources are in the images. Figure 5 shows the results for the high-density image without noise, while Figure 6 shows the results for the high-density image with noise.

These results show the power of the method, and also demonstrate that it is relatively straightforward to implement in HIPE.

4 Plan for implementation

For full implementation of the method, the following gives an estimated costing.

1. Capture requirements (including how to give information about covariance between close pairs or groups of sources): **2 days**.
2. Implement conjugate gradient method for matrix inversion, for speed and so that larger segments of the map can be processed at once (using either `herschel.ia.numeric.toolbox.fit.ConjugateGradientFitter` or `herschel.ia.toolbox.mapper.Pcg` or adapting Fortran code from HerMES or coding from scratch). **4 days**.
3. Implementation of algorithm, with test harness: **5 days**.
4. Wrap computation in a HIPE Task, with conversion from and to world coordinates: **2 days**.
5. Testing, including optimal parameters for segmentation of the map, considering computational/memory limits: **3 days**.
6. Documentation: **2 days**.

Total: **18 days**.

5 Conclusion

The linear inversion methods have been investigated and tested with a prototype. The methods are powerful, simple, and feasible to implement within HIPE.

References

- Berta S., et al. (2010). Dissecting the cosmic infra-red background with Herschel/PEP. *A&A*, 518:L30, 1005.1073.
- B  thermin M., Dole H., Cousin M., Bavouzet N. (2010). Submillimeter number counts at 250 μm , 350 μm and 500 μm in BLAST data. *A&A*, 516:A43, 1003.0833.
- Chapin E. L., et al. (2011). A joint analysis of BLAST 250-500 μm and LABOCA 870 μm observations in the Extended Chandra Deep Field-South. *MNRAS*, 411:505–549, 1003.2647.
- Magnelli B., Elbaz D., Chary R. R., Dickinson M., Le Borgne D., Frayer D. T., Willmer C. N. A. (2009). The $0.4 < z < 1.3$ star formation history of the Universe as viewed in the far-infrared. *A&A*, 496:57–75, 0901.1543.

- Roseboom I. G., et al. (2010). The Herschel Multi-Tiered Extragalactic Survey: source extraction and cross-identifications in confusion-dominated SPIRE images. *MNRAS*, 409:48–65, 1009.1658.
- Scott S. E., et al. (2002). The SCUBA 8-mJy survey - I. Submillimetre maps, sources and number counts. *MNRAS*, 331:817–838, arXiv:astro-ph/0107446.

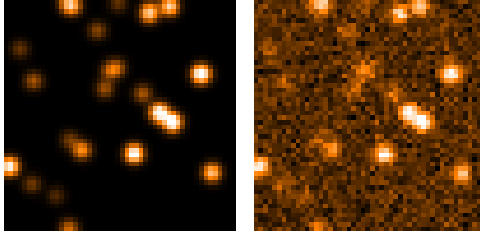


Figure 1: Images for the low-density test, with no noise (left) and with noise (right).

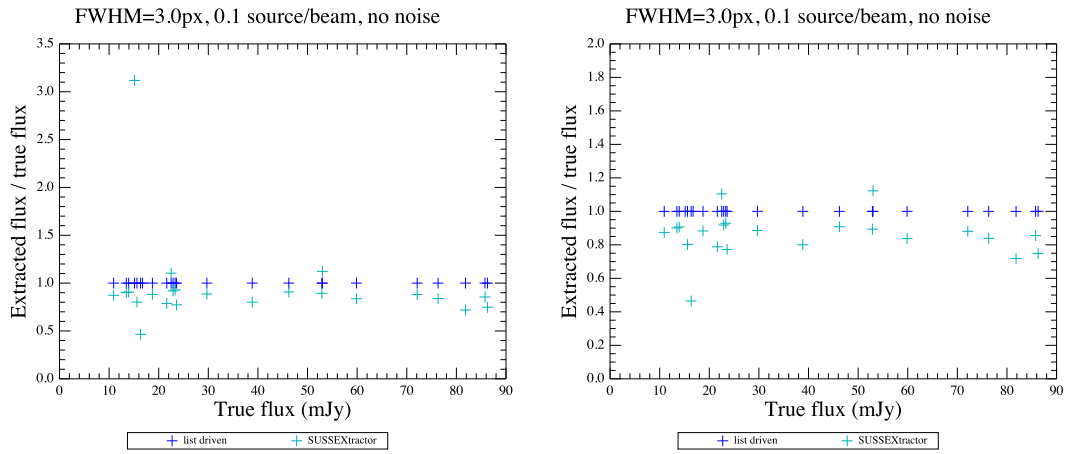


Figure 2: Results for the low-density test, on the image with no noise. The right-hand plot shows the central part of the left-hand plot.

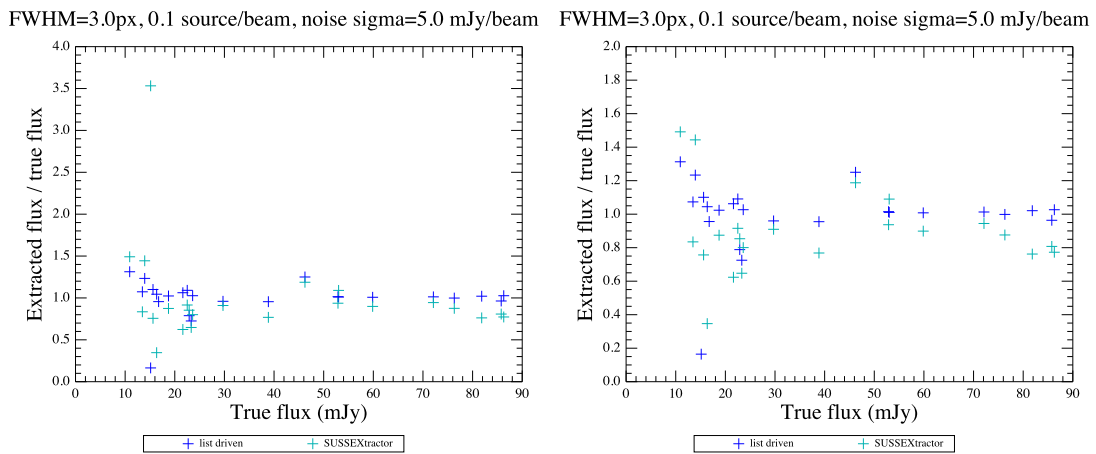


Figure 3: Results for the low-density test, on the image with noise. The right-hand plot shows the central part of the left-hand plot.

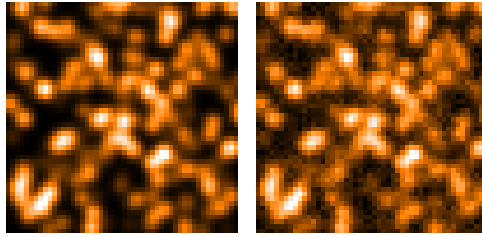


Figure 4: Images for the high-density test, with no noise (left) and with noise (right).

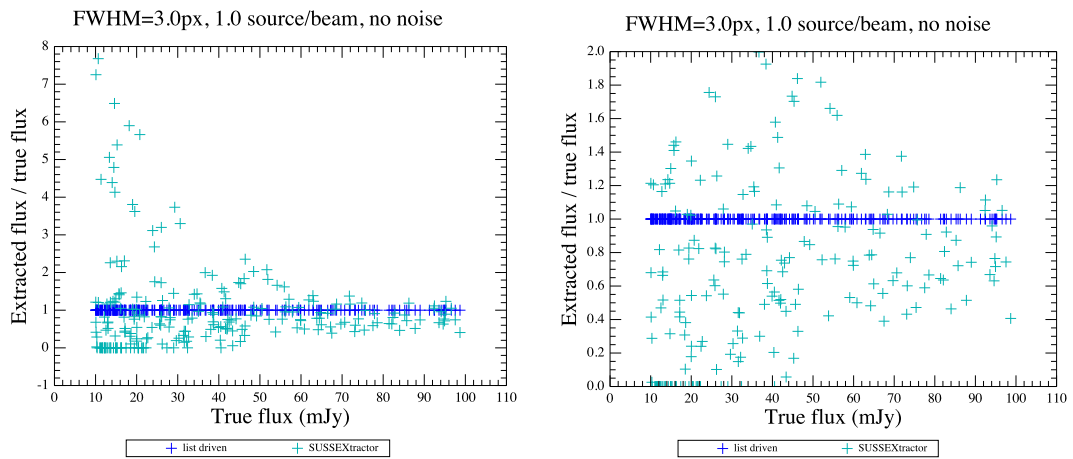


Figure 5: Results for the high-density test, on the image with no noise. The right-hand plot shows the central part of the left-hand plot.

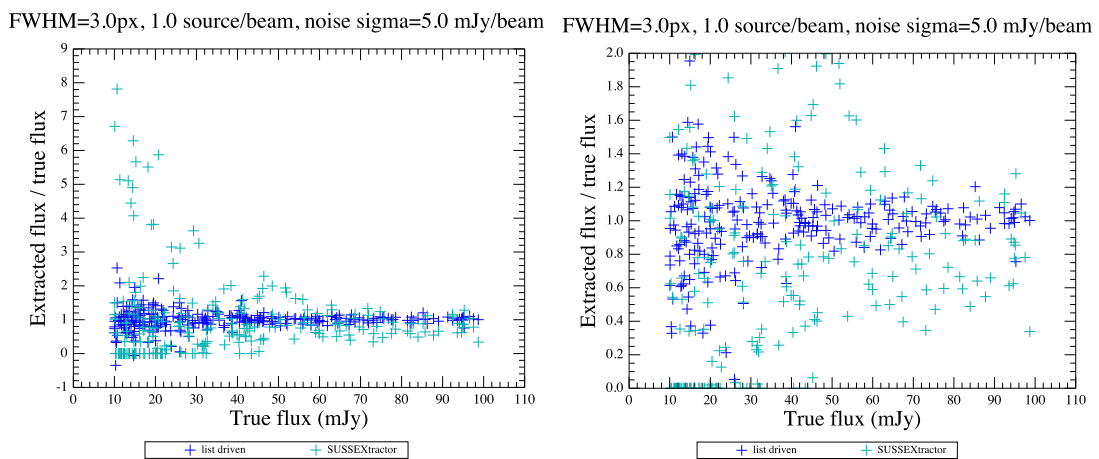


Figure 6: Results for the high-density test, on the image with noise. The right-hand plot shows the central part of the left-hand plot.